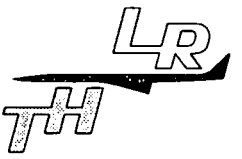

DELFT UNIVERSITY OF TECHNOLOGY

DEPARTMENT OF AEROSPACE ENGINEERING

Report LR - 240

INTERNAL FATIGUE CRACKS ARE GROWING IN VACUUM

by

J. Schijve

DELFT - THE NETHERLANDS

January 1977

DELFT UNIVERSITY OF TECHNOLOGY

DEPARTMENT OF AEROSPACE ENGINEERING

Report LR - 240

INTERNAL FATIGUE CRACKS ARE GROWING IN VACUUM

by

J. Schijve

DELFT - THE NETHERLANDS

January 1977

ABSTRACT

Cylindrical specimens of 2024 and 7075 Al alloy material were heat treated with a cold water quench to obtain high residual tensile stresses at the interior. Fatigue tests showed internal cracks growing in the shear mode. By drilling a hole along the centre line internal cracks were given access to air, which then produced tensile mode cracks. Prestraining of specimens eliminated residual stresses thus producing crack initiation at the outer surface with crack growth in the tensile mode. Cracking in the tensile mode was sensitive to mean stress, whereas cracking in the shear mode was not. The shear mode crack on a micro level appeared to be slip band cracking.

CONTENTS

1. INTRODUCTION

Fatigue cracks usually start at the outer surface of a material for several reasons:

(1) Inhomogeneous stress distributions always imply a higher stress at the surface.

(2) Fatigue resistance of a material will be lower at the material surface. This can be due to geometrical effects (machining, roughness etc.) or to the material structure being more prone to crack initiation.

(3) At the outer surface the environment may contribute to the nucleation of micro cracks.

However, there are exceptions to crack initiation at the surface. Two sources for sub-surface initiation are material defects and suitable residual stress distributions. In such cases the crack nucleation and initial growth of the internal fatigue crack occur under vacuum conditions.

It was indicated by Vogelesang (Refs. 1, 2) that fatigue mode failures in humid air on one hand and in vacuum on the other are significantly different. In humid air water vapour as an aggressive agent will enhance crack growth, while also promoting the tendency to grow perpendicular to the main principal stress. In vacuum, however, crack growth is largely dependent on plastic slip only, which stimulates the crack to grow under shear angles to the main principle stress. As pointed out by Vogelesang a unique relation between growth in the tensile mode under plane strain conditions and growth in the shear mode in plane stress conditions is invalid. This should have consequences for the growth of fatigue cracks initiated at sub-surface locations in view of the fact they would be growing in vacuum.

In the present investigation crack initiation at the centre line of cylindrical specimens was obtained as a result of residual tensile stresses. The stresses were introduced by quenching in cold water after solution heat treatment of specimens machined from 2024-T3 and 7075-T6

material. A comparison is made between the fracture mode of internal cracks growing in vacuum and fracture modes of the same specimens with full access of the environment (air) to the nucleation site and the growing crack. A survey of experiments and results will be given with a short discussion.

2. SPECIMEN PREPARATION

Internal fatigue crack initiation requires residual compressive stresses at the outer surface and residual tensile stresses away from the surface. Two methods to produce such stresses were employed in some initial trials, viz. (1) surface rolling and (2) preloading of notched specimens followed b a remachining to an unnotched configuration. These methods were partly successful, but crack initiation at the centre line of the specimen was not obtained. More success was achieved by a solution treatment with a rapid quench in cold water. Cylindrical specimens as shown in figure 1 were machined from 7075-T6 and 2024-T3 plate material of 25 and 20 mm thickness respectively. After machining an additional heat treatment was carried out as shown below.

	Solution treatment	Quench	Ageing
7075-T6	480°C, 60 minutes	Cold water (5°C)	120°C, 24 hours
2024-T3	495°C, 60 minutes	ditto	Roomtemperature, > 4 days

Mechanical properties of the two alloys before and after the heat treatment including initial parts of the stress-strain curves are presented in figure 2, which will be discussed later.

Specimens with the above heat treatment exhibited crack nucleation in the centre line. In order to prove that nucleation was caused by residual tensile stresses a number of specimens were prestrained to remove the residual stresses. This was done by applying a 3.5 percent plastic strain to the 7075 specimens and 5 percent plastic strain to the 2024 specimens. The prestrain was applied after the heat treatment and before the fatigue test. Crack nucleation then occurred at the outer surface of the specimens.

Other specimens, not prestrained, were provided with a small axial hole drilled along the centre line (see Fig. 1b). The purpose of the hole was

to give access of the environment to the centre of the specimen. In this way it could be ascertained whether the mode of failure of a crack starting at the centre line would be affected by the environment. The hole diameter was 1.6 mm and drilling such a long hole requires a careful operation. In one specimen it was done by spark erosion, but in all other specimens it occurred by mechanical drilling.

3. FATIGUE TEST RESULTS

The residual stress distribution caused by quenching will follow the picture shown in figure 3, taken from Forrest (Ref. 3), who quotes several data from older sources.
In order to avoid the risk of a stress redistribution during fatigue testing most tests were carried out at zero mean stress. Later it was thought to be still interesting to see the effect of mean stress on fatigue life for the two modes of failure observed. Therefore a small number of tests were carried out at positive mean stress.

All specimens were tested at ambient temperature in an Amsler electro-hydraulic testing machine with a 20 tons maximum capacity. The load frequency was 20 Hz. A survey of the fatigue tests and the results are given in the tables in the Appendix.
Fatigue lives for the two alloys have been plotted in figures 4 and 5 respectively.
Three different types of failure were observed as shown in figures 6 and 7.

(a) Shear mode failures starting at the centre line of the specimen (fig. 6)
(b) Tensile mode failures starting at the outer surface (fig. 7, left).
(c) Tensile mode failures starting at the small hole along the centre line (fig. 7, right).

Shear mode failures. This type of failure only occurred in specimens with residual tensile stresses causing crack nucleation at the centre line. The crack growing in vacuum is growing under an oblique angle to the axis of the specimen. The angle was fairly close to 45^{o} for the 2024 alloy, whereas it was somewhat smaller for the 7075 alloy. The macroscopic orientation of the fracture plane was always similar with respect to the axes of the plate from which the specimens were taken with the fracture plane being parallel to the long transverse direction. Crack growth apparently occurred more or less in a concentric way, since the final failure area was never highly excentric (see fig. 6 for the

7075 alloy). This observation is easily understood by considering the rotational symmetry of the residual stress distribution with compressive stresses at the outer surface.

Tensile mode failures. This type of failure staring at the outer surface occurred in all prestrained specimens and in three unprestrained 2024 specimens loaded at high stress amplitudes. Tensile mode failures starting at the small hole in the centre line were observed in all unprestrained specimens with such a hole. In other words tensile mode failures occurred in all cases were the air environment has access to the crack. If this did not apply the crack was growing in vacuum and a shear mode failure was found. In the specimens with residual stresses and the central hole crack growth again occurred in a concentric way, see figure 7a, right.

A 7075 specimen with a shear mode failure was sectioned longitudinally over its full length. A second crack with a length of 2.5 mm was found which is shown in figure 8, confirming its shear mode character.
Two 2024 specimens were also sectioned but a second crack was not found. Cross sections of the main fracture indicated that slip band cracking occurred in the 7075 specimens. A similar indication for the 2024 specimens was less clear.

4. DISCUSSION

Residual stresses

G. Forrest explained how inhomogeneous cooling during quenching can produce residual compressive stress at the surface and residual tensile stress in the interior (Ref. 3). For cylindrical bars of two Al-Cu alloys quenched in cold water he quotes maximum residual tensile stresses of 177 and 117 N/mm^2 respectively with a distribution as shown in figure 3. A first estimate of the maximum residual stress in the present investigation can be obtained from figure 2. The apparent elastic limit of the material with residual stresses will be reached if the stress at the centre line of the cylindrical specimen exceeds the true elastic limit of the material.

The latter limit is now assumed to be still equal to the elastic limit of the original material. As a consequence the apparent reduction of the elastic limit after quenching will be equal to the residual tensile stress of the centre line. The reductions are indicated in figure 2 by arrows. The maximum residual stresses estimated in this way are equal to 200 N/m^2 for the 7075 alloy and 140 N/mm^2 for the 2024 alloy. These values agree with the order of magnitude given by Forrest. The magnitude of the residual compressive stress at the outer surface will probably be smaller than the above values but the difference between the residual tensile stress at the centre line and the residual compressive stress at the surface will anyhow be larger. As a result there will be a most significant difference between the cyclic stress ranges at the centre line and the outer surface. In figure 3 this is illustrated by dotted lines applicable to $\sigma_m = 0$. It very well explains why crack initiation is prevented at the surface, whereas it is enhanced at the centre line. All quenched specimens showed crack initiation at the centre line, except for three specimens of the 2024 alloy tested at high stress amplitudes. It is thought that the maximum stress at the centre line in these specimens exceeded the elastic limit, causing a redistribution of the residual stress with a possibility of further cyclic plastic shake

down during the fatigue test.

The effect of the residual stress distribution on crack nucleation at the centre line was substantiated by tests on prestrained specimens. Since prestraining occurred well into the plastic range of the σ-ε curve it will have eliminated the residual stresses almost completely. The intersecting S-N curves (fig. 4) of the prestrained and unprestrained material is the result of different effects. Without prestrain the maximum stress in the specimen will be considerably higher at the centre line due to residual stresses. This will enhance crack nucleation. It also might accelerate crack growth, however, the crack will grow in vacuum which may imply a much slower crack rate than in air. At the same time the cracking mechanism also appears to be different as discussed later.

Specimens with residual stresses and a small hole along the centre line do not have the benefit of crack growth in vacuum, while the disadvantage of residual tensile stresses is still present. The residual stresses will promote early crack initiation and crack growth. As a result inferior S-N curves have to be expected (fig. 4).

Only a few fatigue tests were carried out with a positive mean stress. A significant reduction of the fatigue life was found for the prestrained specimens (fig. 5). This reflects the well known effect of mean stress on life if no residual stresses are present. Surprisingly enough the effect of mean stress was quite small for the specimens with residual stresses. Since crack initiation still occurred at the centre line, it is possible that crack growths in vacuum is much less sensitive to mean stress as suggested by the model discussed by Vogelesang (Refs. 1,2). It may also be thought that exceeding the elastic limit at the centre line will reduce the effect of mean stress. Three mean stresses were used, viz. 0, 123 and 196 N/mm^2. With a residual tensile stress at the centre line estimated at 200 N/mm^2 and a stress amplitude of 123 N/mm^2 the maximum stresses at the centre line are 323, 446 and 519 N/mm^2.
Thus according to the σ-ε curve of the original material a redistribution

need not be expected.

The mode of failure

The specimens of both alloys (2024 and 7075) indicated a unique relation between the two modes of failure and the two environments. Internal cracks growing in vacuum invariably produced shear mode failures, whereas crack growth in air always occurred in the tensile mode. The latter applied both to cracks starting from the outer surface of the specimens and to cracks starting at the centre of the specimen provided that air was available through a small hole along the centre line. These results are strong evidence that fatigue cracks in aluminium alloys prefer to grow macroscopically in the tensile mode in an aggressive environment, whereas growth will occur in some type of shear mode in inert environments (Refs. 1, 2).

Similar shear mode failures as shown in figure 6 were reported by Dudek (Ref. 4) for a 7075 type alloy. He also quenched fully machined specimens in cold water and found many shear type failures. Moreover, he also found that prestraining changed the mode of failure to the tensile mode starting at the outer surface. Surprisingly enough he argues that internal cracking cannot be due to quenching stresses. The explanation offered in Ref. 4 is based on different precipitation structures of the alloy at the surface and in the interior. The shear mode cracking is also based on the same argument. It appears that the present results, especially those obtained on specimens with a small hole along the centre line, fully rule out this explanation.

In agreement with the present observation Dudek (Ref. 4) found that a shear mode crack progressed along slip planes. Pictures like figure 8 suggest the concept of "slip band cracking" which may be associated with Stage I fatigue-crack growth as defined by Forsyth (Ref. 5). Stage I cracking is supposed to occur in the early stages of micro-crack growth and possibly also later on if crack growth is very slow due to low stress

levels. In a recent study Nageswararao, Kralik and Gerold (Ref. 6) also found that slip band cracking was promoted by vacuum and a low stress amplitude. In the present study, however, shear mode failures were also obtained at high stress amplitudes with low endurances, even as low as 35,000 cycles, which implies high crack rates. It is thought that slip band cracking could still occur in view of the absence of any aggressive agent, which otherwise would have produced a tensile mode failure. This view is supported by the tests at positive mean stresses (fig. 5) where fatigue cracking still occurred in the shear mode. At the same time it should be noted that the vacuum condition is not in itself an explanation for the observed slip band cracking, although it was a required condition in the present tests.

The shear mode crack growth persisted in a single macroscopic shear plane with a fixed orientation to the original plate from which the specimens were cut. It is expected that texture must have been of some importance in this respect. However, another aspect should not be overlooked. If the very first internal crack has been nucleated early in the life along a slip plane, making an oblique angle to the specimen axis, it will cause shear stress concentrations in its own plane. This may well lead to concentrated cyclic slip on slip planes making small angles with the plane of the crack. It then should be expected that crack growth in new grains prefer to occur on planes in line with the crack. The same could apply to crack nucleation at the outer surface in an air environment (stage I nucleation). However, crack extension in terms of decohesion is also sensitive to tensile stresses due to environmental effects. According to the model proposed in Refs. 1 and 2 cracks should then be expected to grow perpendicular to the main principal stress.

5. CONCLUSIONS

Fatigue tests were carried out on unnotched cylindrical specimens of 2024 and 7075 Al alloy material. The specimens, after machining, were given a new heat treatment including quenching in cold water. The purpose was to introduce high residual tensile stresses in the interior and residual compressive stresses at the outer surface in order to obtain fatigue crack nucleation inside the material with subsequent crack growth in vacuum. The results are summarized below:

(1) Values of the residual tensile stress of the centre line of the specimens were estimated to be 140 N/mm^2 (20,300 psi) for the 2024 alloy and 200 N/mm^2 (29,000 psi) for the 7075 alloy. The estimates were based on stress-strain curves.

(2) As a result of its residual stresses crack nucleation occurred at the centre line of the specimen which was followed by concentric crack growth to the outer surface.

(3) If residual stresses were removed by prestraining crack nucleation occurred at the outer surface.

(4) Internal cracks growing in vacuum exhibited macroscopically a shear mode fracture under an angle of about 45 degrees to the loading direction for the 2024 alloy specimens and a somewhat smaller angle for the 7075 alloy specimens. On a microscopic level crack growth appeared to be slipband cracking.

(5) Internal cracks growing in air could be obtained by drilling a hole with a small diameter along the centre line. These cracks were macroscopically growing as a tensile mode fracture in a plane perpendicular to the loading direction. Cracks starting from the outer surface (after prestraining) were tensile mode fractures also.

(6) Apparently there was a unique correlation between tensile mode fatigue fractures in air and shear mode fractures in vacuum. This implies a different cracking mechanism for the two environments. A small number of tests indicated that the tensile mode fracture was sensitive to the mean stress of the cyclic load, whereas the shear mode fracture was not.

6. ACKNOWLEDGEMENT

The fatigue tests were carried out by J. Snijder, the heat treatments and the microscopical work by R. Elenbaas. Their careful help is greatly appreciated.

7. REFERENCES

1. L.B. Vogelesang - Some aspects of the environmental effect on the fatigue mechanism of a high stregth aluminium alloy. Proc. 8th ICAF Symp., Lausanne 1975, Swiss Federal Aircr. Est. (also Delft Un. of Technology, Report VTH-200).
2. L.B. Vogelesang - Some factors influencing the transition from tensile mode to shear mode under cyclic loading. Delft University of Technology, Report LR-222, Aug. 1976.
3. G. Forrest - Internal or residual stresses in wrought aluminium alloys and their structural significance. J. of the Royal Aero. Soc., Vol. 58, 1954, 261-276.
4. H.J. Dudek - Einfluss des Ausscheidenszustandes auf die Ermüdungs-bruchfläche bei der Legiering AlZnMgCu 1.5 (Influence of age conditions on the fatigue fracture surface of the aluminium alloy 7075). DFVLR Report DLR-FB 73-100, Porz-Wahn 1973.
5. P.J.E. Forsyth - The physical basis of metal fatigue. Blackie & Son, London 1969.
6. M. Nageswararao, G. Kralik and V. Gerold - Slip band cracking at low fatigue crack growth rates in two Al-Zn-Mg alloys. Z. Metallkunde, Vol. 66, 1975, 479-486.

APPENDIX: TEST RESULTS

σ_a and σ_m in N/mm^2

Conditions: No prestrain and σ_m = 0							
7075				2024			
Specimen	σ_a	N	Failure (a)	Specimen	σ_a	N	Failure (a)
1	245	60380	S	4	245	89850	T
2	216	34800		5	216	220480	
5	200	133660		8	216	238650	
3	177	244720		3	196	360670	S
10	177	296210		6	177	673540	
6	147	372950		7	147	1141250	
7	128	642310		9	118	5001340	
8	118	713590					
16	108	4249940					
15	98	9453250					

a) S = shear mode failure, starting in centre of specimen
T = tensile mode failure, starting at surface of specimen
T_h = tensile mode failure, starting at axial hole

Conditions: Prestrained and σ_m = 0							
7075 (3.5% prestrain)				2024 (5% prestrain)			
Specimen	σ_a	N	Failure (a)	Specimen	σ_a	N	Failure (a)
11	245	42390	T	14	245	59050	T
4	177	129960		15	216	63190	
9	147	536510		11	177	62850	
13	128	>2311830		16	157	206230	
26	123	6873170		10	147	318930	
				13	147	608230	
				18	132	2801740	
				12	118	>15898520	

Conditions: No prestrain, axial hole, $\sigma_m = 0$							
7075				2024			
Specimen	σ_a	N	Failure (a)	Specimen	σ_a		Failure (a)
12	147	74230		19	118	191620	T_h
6'	147	93290		20	98	584330	T_h
18	118	135390	T_h	17	88	>4185000	
19	98	153270					

Condition: $\sigma_m > 0$					
Material	Prestrain	Specimen	$\sigma_m \pm \sigma_a$	N	Failure (a)
7075	No	14	123 ± 123	616790	S
	No	21	123 ± 123	710000	
	No	22	196 ± 123	559620	
	Yes (3.5%)	24	123 ± 123	2069420	T
	Yes (3.5%)	25	196 ± 123	448710	

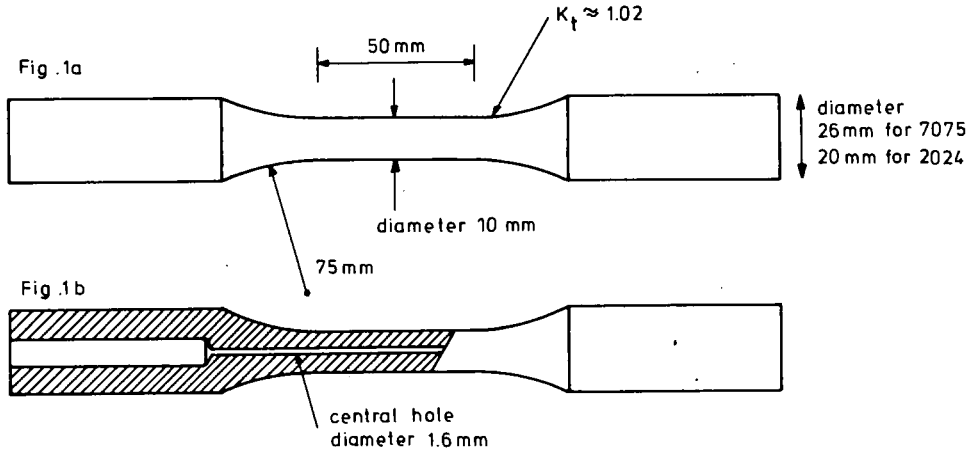

Fig. 1. Specimens.

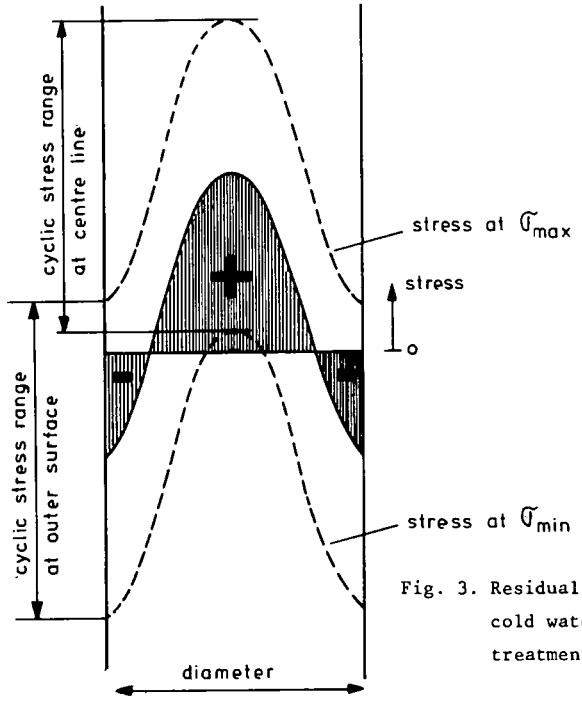

Fig. 3. Residual stress distribution after cold water quench from solution heat treatment temperature.

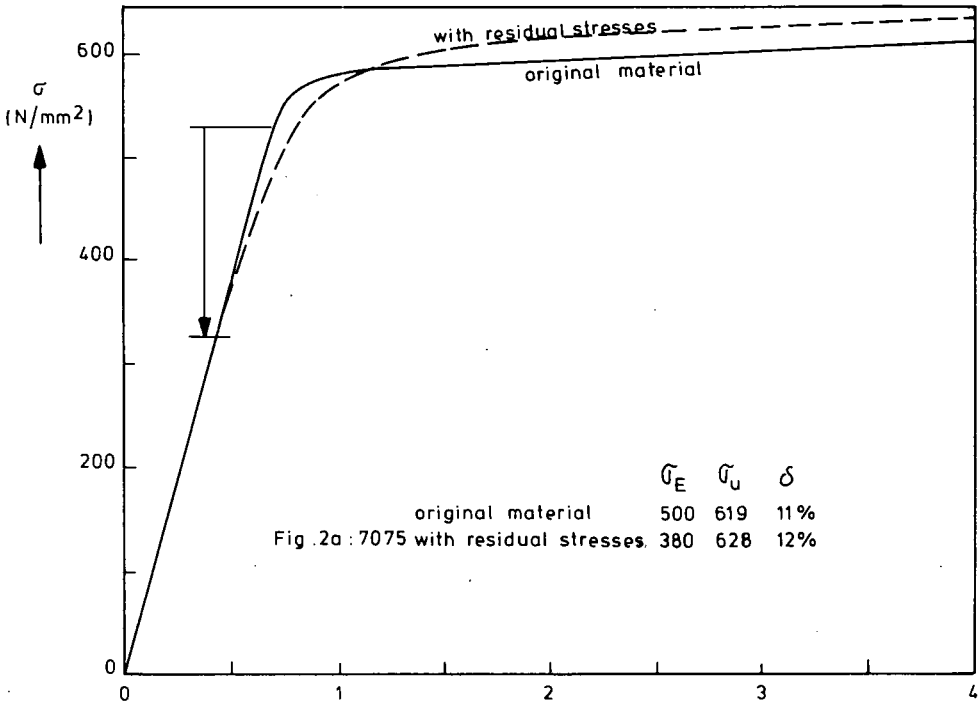

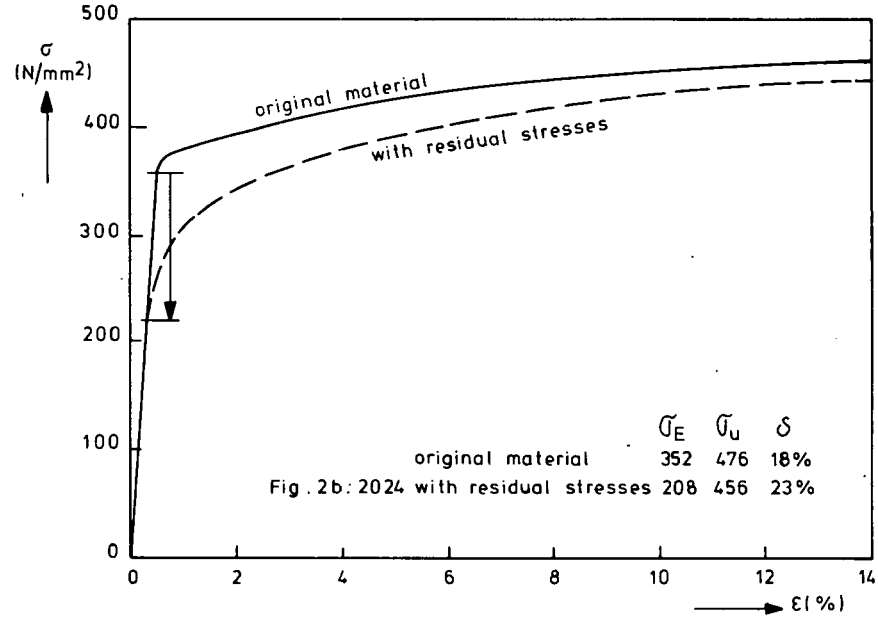

Fig. 2. Stress-strain curves.

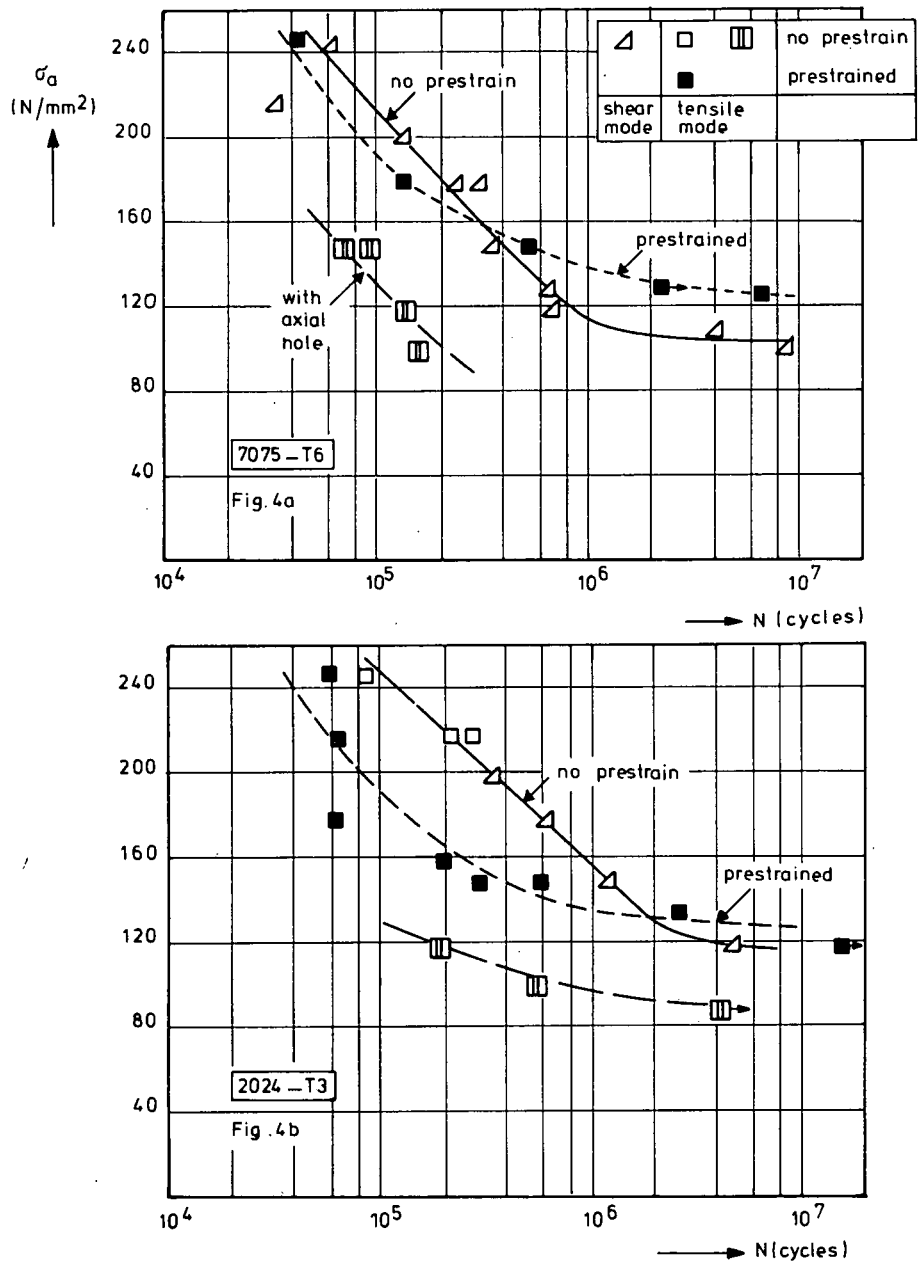

Fig. 4. The S-N curves for 7075-T6 and 2024-T3 specimens, $\sigma_m = 0$.

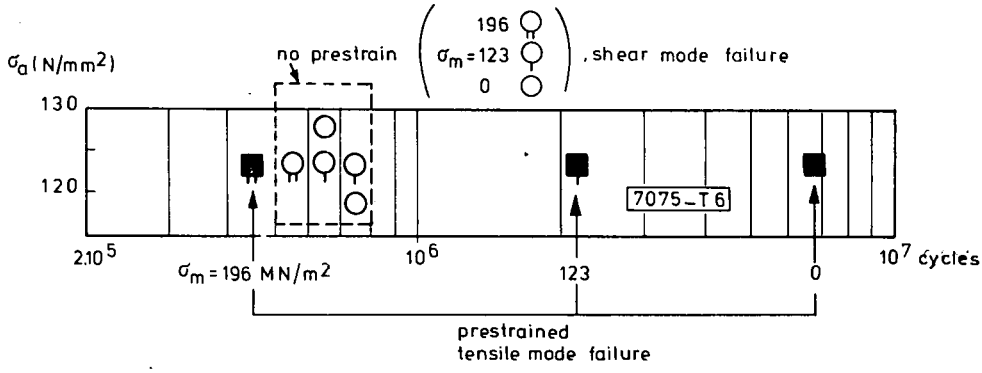

Fig. 5. The effect of mean stress (σ_m) on fatigue life of specimens without prestrain (internal shear mode failure) and with prestrain (external tensile mode failure).

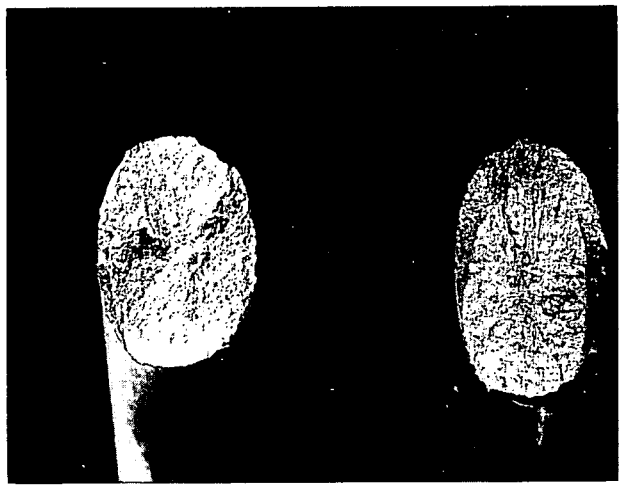

Fig .6a

neg.76–224

2024–T3
no prestrain
σ_a = 196 MN/m^2
N = 360 670

7076–T6
no prestrain
σ_a = 123 MN/m^2
N = 616 790

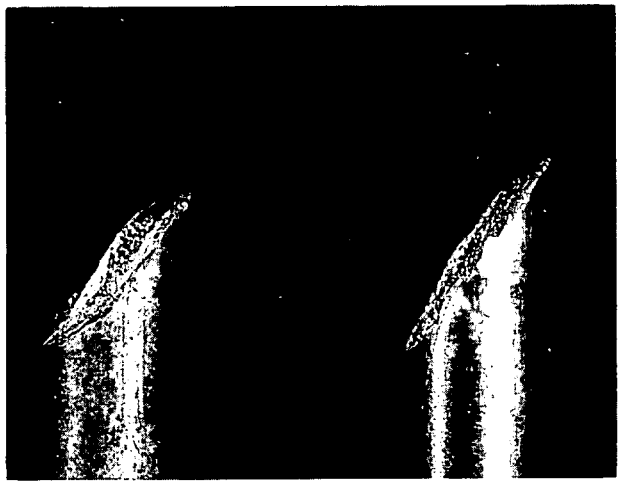

Fig .6b

neg .76–225

Fig. 6. Two specimens with shear mode fatigue failures, which nucleated at the center of the specimen (magnification 2.4 x).

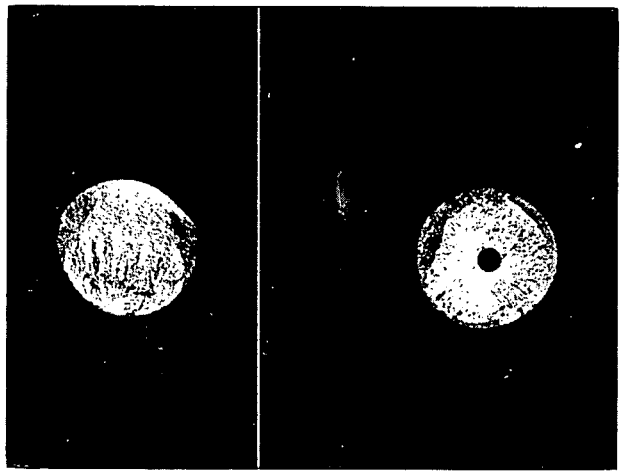

7075 – T6
prestrained 3,5 %
σ_a = 147 MN/m^2
N = 536 510

7075 – T6
no prestrain
σ_a = 118 MN/m^2
N = 135 390

Fig .7a

neg . 76–226

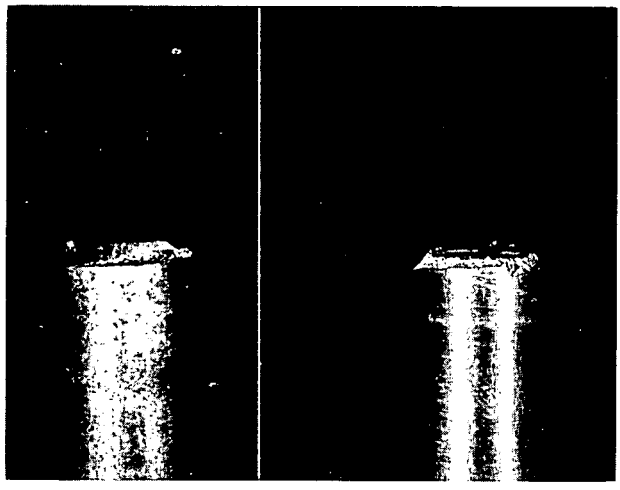

Fig .7b

neg .76 – 227

Fig. 7. Two specimens with tensile mode fatigue failures, which nucleated at the outside surface (left) or the axial hole (right) (Magnification 2.2 x).

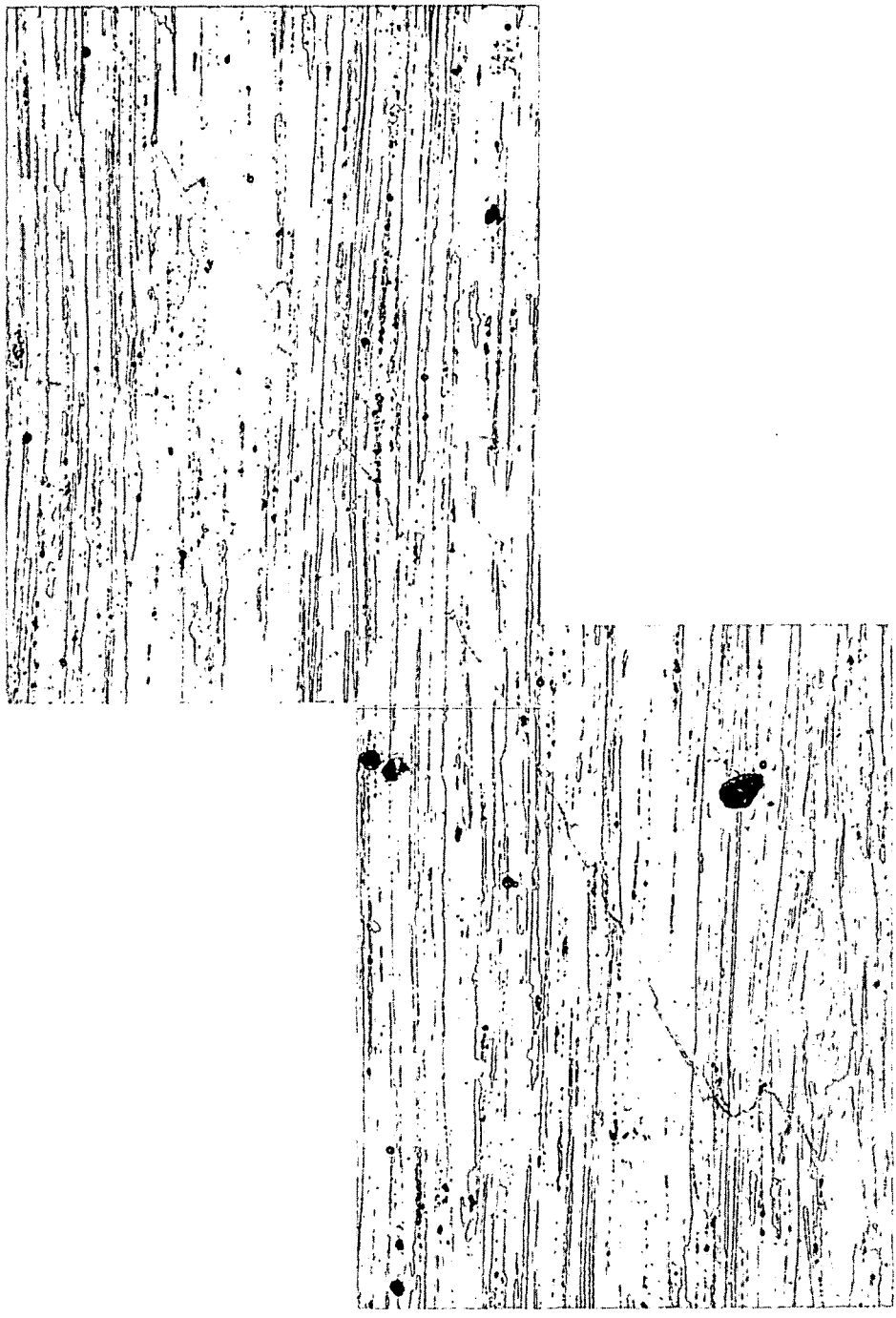

Fig. 8. Cross section of an internal crack in a 7075-T6 specimen (No. 5, N = 133660 cycles). Magnification 80 x.